Synthesis and Characterization of Platinum Catalysts on Multiwalled Carbon Nanotubes by Intermittent Microwave Irradiation for Fuel Cell Applications

Zhi Qun Tian,[†] San Ping Jiang,*[,†] Yong Min Liang,[‡] and Pei Kang Shen[§]

School of Mechanical and Aerospace Engineering, Nanyang Technological University, Singapore 639798, Fuel Cell Engineering Centre, Dalian Institute of Chemical Physics, Chinese Academy of Sciences, Dalian 113023, China, and School of Physics and Engineering, Sun Yat-Sen University, Guangzhou 510275, China

Received: November 5, 2005; In Final Form: December 29, 2005

Pt electrocatalysts supported on multiwalled carbon nanotube (Pt/MWCNT) nanocomposites have been synthesized by a rapid intermittent microwave irradiation (IMI) technique for polymer electrolyte and direct methanol fuel cells (PEFCs and DMFCs), using H_2PtCl_6 as Pt precursor. The Pt/MWCNT nanocomposites are characterized by XRD, XPS, and TEM. The results indicate that Pt particle size and distribution on the MWCNT support are affected significantly by the oxidation treatment of MWCNTs, the IMI procedure, and the MWCNT tube diameter or surface area. The PtO_x ($x = 1, 2$) species was first deposited on the surface of MWCNTs by the IMI and subsequently reduced to Pt(0) with refluxing in the presence of HCOOH. Pt/MWCNT nanocomposites synthesized by this IMI method have achieved extremely uniform dispersed Pt nanoparticles with a particle size of ∼3 nm. Electrochemical measurement indicates that Pt/MWCNT nanocomposites synthesized by the IMI method display a significantly higher electrochemically active area and higher catalytic activity for the methanol oxidation reaction in comparison to a commercial Pt/C catalyst.

1. Introduction

Polymer electrolyte and direct methanol fuel cells (PEFCs and DMFCs) are the most promising power sources for applications such as electric vehicles and electronic portable devices, due to their high power density, relatively quick start-up, rapid response to varying loading, and low operating temperature.[1] Nanosized platinum and platinum alloy supported on carbon black are the most important electrocatalysts in these fuel cells.[2] However, one of the most significant barriers for the widespread commercialization of PEFCs and DMFCs is the high cost of precious Pt and Pt alloy catalyst. It is important to reduce the amount of precious metal catalyst and thus the overall cost of the fuel cell. One way to achieve this goal is by using high surface area carbon support (e.g., Vulcan XC-72 carbon black) to enhance the dispersion of metal nanoparticles and thus to increase the utilization of the precious metal catalyst.[3−5]

Carbon nanotubes (CNTs) with unique electrical and structural properties have attracted great interest in applications such as superconductivity, hydrogen storage, field emission, and heterogeneous catalysis.[6−11] CNTs are also widely studied as support for Pt and Pt alloy catalysts in PEFCs and DMFCs due to the high surface area, excellent electronic conductivity, and high chemical stability.[12−22] However, deposition, distribution, and crystallite size of Pt nanoparticles supported on CNTs are significantly affected by factors including the synthesis method, oxidation treatment of the CNTs, and the Pt precursors. Liu et al.[17] prepared Pt catalysts on multiwalled carbon nanotubes (Pt/MWCNTs) by electroless plating facilitated by a two-step sensitization−activation pretreatment. The Pt/MWCNT electrocatalysts with 67.3% of Pt(0) and 32.7% of Pt(IV) showed reasonable activity. However, agglomeration of Pt nanoparticles was observed. Mu et al.[21] prepared Pt/MWCNT nanocomposites by impregnation and heat treatment in H_2 at 400 °C, and the deposited Pt was characterized by the formation of clusters which were as large as 50 nm. Tang et al.[22] deposited Pt catalysts on well-aligned carbon nanotubes by a potential-step method and observed higher electrocatalytic activity for oxygen reduction reaction in comparison with Pt/graphite electrode. Han et al.[23] used an alcoholic reduction method to deposit Pt catalysts on CNT supports. The size of the Pt nanoparticles varied from 3 to 10 nm, depending on the concentration of nitric acid solution used for the oxidation treatment of CNTs. Recently, Lin et al.[24] synthesized Pt/CNT nanocomposites in supercritical carbon dioxide fluid using Pt(II) acetylacetonate as metal precursor. The Pt particle size was in the range of 5−10 nm and exhibited reasonbale electrocatalytic activity for methanol oxidation and oxygen reduction reactions. The aforementioned studies indicate that synthesis of highly dispersed and nanosized Pt catalysts supported on carbon nanotubes still remains a challenge. Achieving a high degree of dispersion of Pt catalyst on CNT support is important in order to fully utilize the advantages of high surface area, conductivity, and porosity of CNT-based materials.

Microwave irradiation through a dielectric heating loss permits rapid conversion of precursor/carbon composites to the desired nanocomposites under appropriate conditions. Boxall et al.[25] prepared PtRu/carbon nanocomposites by microwave irradiation using (η-C_2H_4)(Cl)Pt(μ-Cl)$_2$-Ru(Cl)(η^3:η^3-2,7-dimethyloctadienediyl) as a noncluster. The PtRu/C nanocomposites with 50 wt % of PtRu showed a much higher catalytic performance in comparison to that of the E-TEK PtRu/C catalyst. Liu et al.[26] synthesized Pt and PtRu catalysts on carbon support using a microwave-assisted polyol process using thiol-encapsulated metal colloids. The thiol stabilizers have to be removed by heat treatment before the Pt and PtRu supported

* Corresponding author. E-mail: mspjiang@ntu.edu.sg.
[†] Nanyang Technological University.
[‡] Chinese Academy of Sciences.
[§] Sun Yat-Sen University.

10.1021/jp056401o CCC: $33.50
Published on Web 02/21/2006

on carbon can be used as catalyst for fuel cells. Recently, we proposed a rapid synthesis method based on an intermittent microwave irradiation (IMI) technique for preparing Pt catalyst supported on carbon.[27] Uniform Pt catalysts supported on carbon with particle size <5 nm and Pt loading up to 60 wt % were prepared by the IMI method.[28] WC and CeO_2 supported on carbon have also been successfully synthesized by this method.[29,30] In this work, we report the synthesis of Pt supported on multiwalled carbon nanotube (Pt/MWCNT) nanocomposites by the IMI technique. The factors influencing the synthesis, deposition, and dispersion of Pt nanoparticles on MWCNTs are investigated. The Pt/MWCNT nanocomposites are characterized by XPS, XRD, and TEM, and the electrocatalytic activity of the synthesized Pt/MWCNT nanocomposites for the methanol oxidation reaction is studied.

2. Experimental Section

2.1. Oxidation Treatment of MWCNTs. Multiwalled carbon nanotubes (MWCNTs) with different tube diameters of <10 nm, 20−40 nm, and 40−60 nm and purity of >95% were purchased from Shenzhen Nanotech Port Co., Ltd., in China. Two different acid solutions were used for the oxidation treatment of MWCNT supports, following the procedure reported in ref 31. One portion of MWCNTs was treated by H_2SO_4/HNO_3 solution; 1.0 g of MWCNTs was mixed with 100 mL of a 98% H_2SO_4/65% HNO_3 (1:1, v:v) solution under constant stirring for 15 min and then refluxed at 140 °C for 4 h. The resulting MWCNT was rinsed thoroughly to neutral with deionized water and dried at 80 °C for 24 h. A second portion of MWCNTs was treated in a 30% H_2O_2/98% H_2SO_4 (1:1, v:v) solution and refluxed, washed, and dried similarly to the steps used in the H_2SO_4/HNO_3 treatment.

2.2. Synthesis of Pt/MWCNT Nanocomposite. Platinum supported on MWCNT (Pt/MWCNT) nanocomposites were synthesized by the intermittent microwave irradiation (IMI) technique. In this technique, 200 mg of MWCNTs was mixed with 10 mL of 2-propanol under ultrasonic treatment for 15 min. Then 6.1 mL of H_2PtCl_6 precursor (22 mg mL^{-1} Pt, Aldrich) was slowly added to the MWCNT dispersion, followed by ultrasonic treatment for 30 min. After evaporation of the solvent the thermal treatment of the sample was accomplished by dielectric loss heating of the MWCNT support using microwave irradiation (Galanz, WD900ASL23-2) at 2.45 GHz and a fixed power level of 900 W. Different microwave heating procedures were used for the Pt/MWCNT nanocomposites. They were 10-s irradiation on and 60-, 80-, 100-, and 120-s irradiation off, respectively. The microwave irradiation procedure was repeated six times. The as-synthesized Pt/MWCNT nanocomposites were reduced as follows. First, the Pt/MWCNT composites were dispersed in formic acid (0.5 M HCOOH, 25 mL). The dispersion was then put into a microwave oven and argon gas was supplied for 15 min to remove oxygen. Then the oxygen-free solution was heated under argon atmosphere in a procedure of 30-s irradiation on and 40-s irradiation off until the sample was completely dried. The Pt content was determined by ICP-AES, and the Pt loading in Pt/MWCNT nanocomposites in this study was kept as 40 wt %.

2.3. Characterization. Surface area measurements of the MWCNT support were performed on an ASAP 2010 surface area and porosity analyzer at a bath temperature of 77.23 K using nitrogen gas as the adsorbate. Surface areas were obtained using the Brunauer−Emmett−Teller (BET) method. The effect of oxidation treatment on MWCNTs was examined by Raman spectroscopy (Renishaw), using He/Ne laser with a wavelength of 633 nm. An X-ray diffractometer, D/Max-IIIA (Rigaku Co., Japan), using Cu $K\alpha_1$ ($\lambda = 1.540\,56$ Å) as the radiation source was used for identification of the crystalline structure and average crystallite size of Pt particles. The tube current and voltage were 25 mA and 35 kV, respectively. The average crystallite size of Pt particles was estimated from the diffraction peak of Pt(220) using the Debye−Scherrer equation:[32]

$$d = 0.9\lambda_{k\alpha1}/\beta \cos \theta_{max} \quad (1)$$

in which d is the average size of the Pt particle, $\lambda_{k\alpha1}$ is the X-ray wavelength (Cu Kα $\lambda_{k\alpha1} = 1.5418$ Å), θ_{max} is the maximum angle of the (220) peak, and β is the full-width at half-maximum in radians.

Transmission electron microscopy (TEM) was performed on the samples with a Philips CM-300 high-resolution system operated at 200 keV. The samples were prepared by dispersing a small amount of the Pt/MWCNT nanocomposites in ethanol with ultrosonication. A drop of the dispersion was deposited onto 400 mesh copper grid and subsequently dried. X-ray photoelectron spectroscopy (XPS) analysis was conducted on a VG ESCALAB MKII spectrometer using an Al Kα- ray source. XPS PEAK software was used to analyze the valence state and distribution of Pt in Pt/MWCNT nanocomposites.

2.4. Electrochemical Measurement. Electrochemical activity of the synthesized Pt/MWCNT nanocmoposites was evaluated using a disk electrode. GA gold disk (0.255 cm^2) was polished by 0.3 μm alumina paste (Alpha Micropolish, U.S.A.) and treated with a $H_2SO_4 + H_2O_2$ solution for 30 min before use. The polished gold disk was used as the substrate for the working electrode; 5.0 mg of Pt/MWCNT was ultrasonically dispersed into 1.0 mL of 2-propanol for 30 min to form a catalyst ink; 30 μL of the catalyst ink was placed on the gold disk and dried at 80 °C for 30 min; 10 μL of Nafion solution (5 wt %, DuPont) was then sprayed on the Pt/MWCNTs catalyst surface to form a protective layer and avoid loss of catalyst during the test. The total Pt loading was 0.235 mg cm^{-2}.

Electrochemical measurements were carried out on a Volta-Lab 80 electrochemical station (Radiometer Analytical, France). A standard three-electrode cell with separate anode and cathode compartments was used. A platinum foil (1.5 cm^2) was used as the counter electrode. A saturated calomel electrode (SCE) was used as the reference electrode, and all potentials reported in this paper are vs SCE. Before measurements, all electrodes were completely activated to a steady state by cyclic voltammetry (50 cycles) in a 1.0 M $CH_3OH + 0.5$ M H_2SO_4 solution at a scan rate of 100 mV s^{-1} and a potential range from −0.2 to 1.0 V vs SCE. The electrochemically active area of Pt/MWCNT composites was measured in a nitrogen saturated 0.5 M H_2SO_4 solution at a scan rate of 50 mV s^{-1} and the activity for the methanol oxidation reaction in a nitrogen saturated 0.5 M $H_2SO_4 + 1$ M CH_3OH solution at a scan rate of 20 mV s^{-1}. All electrochemical experiments were conducted at room temperature. Pt/Vulcan carbon catalyst (Pt/C) having 40 wt % of Pt obtained from E-TEK, Inc., was also tested using identical procedures of electrode preparation and electrochemical activity measurement.

3. Results and Discussion

3.1. Effect of Oxidation Treatments of MWCNTs. Figure 1 shows the TEM micrographs of the Pt/MWCNT nanocomposites prepared on MWCNTs without and with the oxidation treatment in H_2O_2/H_2SO_4 and H_2SO_4/HNO_3 solutions. In the case of Pt/MWCNTs prepared with as-received MWCNTs, the

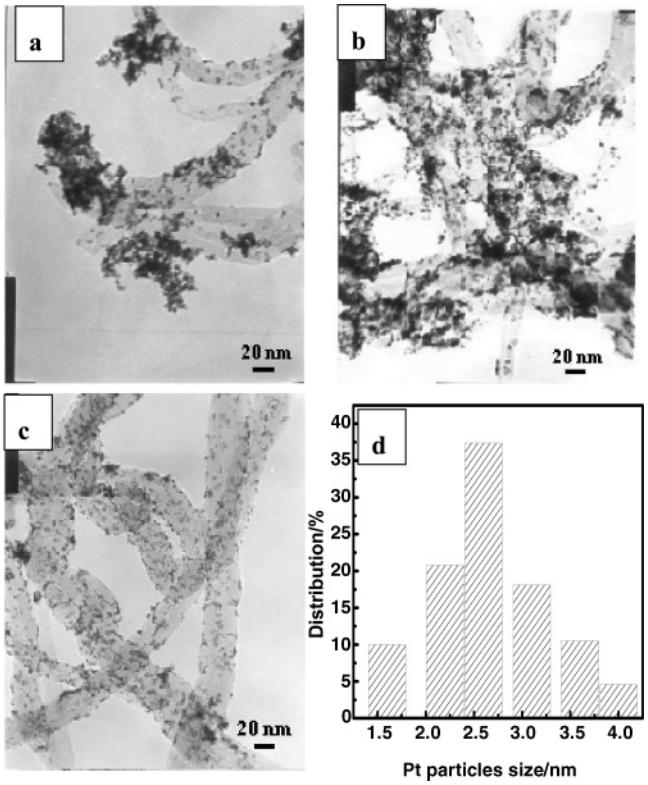

Figure 1. TEM micrographs of the Pt/MWCNT nanocomposites prepared with (a) as-received MWCNTs, (b) MWCNTs treated by H_2SO_4/H_2O_2 solution, (c) MWCNTs treated by H_2SO_4/HNO_3 solution, and (d) histogram of Pt nanoparticle distribution of (c). Pt/MWCNTs were prepared by intermittent microwave irradiation with 10-s irradiation on and 100-s irradiation off, and MWCNTs' diameter was 20−40 nm.

distribution of Pt nanoparticles is not uniform and large Pt clusters were formed on selected areas of the MWCNTs (Figure 1a). After the oxidation treatment by H_2SO_4/H_2O_2 solution, the dispersion of Pt particles on the MWCNTs is improved in comparison to that prepared with as-received MWCNTs (Figure 1b). However agglomerates of Pt nanoparticles are clearly visible. On the other hand, the treatment of MWCNTs in H_2SO_4/HNO_3 significantly improved dispersion and distribution of Pt nanoparticles, as shown in Figure 1c. The Pt/MWCNTs are characterized by a narrow distribution of Pt particles with average particle size of 2.73 ± 0.30 nm (Figure 1d). Pt/MWCNT nanocomposites prepared on MWCNTs without and with different treatments were also characterized by XRD analysis. The average particle size of Pt deposited was measured by the line broadening of the Pt(220) peak using Scherrer's formula. The average size of Pt particles was 4.2 nm, 3.5 nm, and 2.9 nm for the Pt/MWCNTs prepared on as-received, H_2SO_4/H_2O_2 treated, and H_2SO_4/HNO_3 treated MWCNTs, respectively. The results indicate that the oxidation treatment of the MWCNTs is very important for the dispersion and particle size distribution of the Pt/MWCNT nanocomposites synthesized by intermittent microwave irradiation.

The Raman spectra of as-received MWCNTs and MWCNTs treated by H_2O_2/H_2SO_4 and H_2SO_4/HNO_3 solutions are shown in Figure 2. All MWCNT samples have similar Raman scattering patterns. The peak near 2650 cm^{-1} (G′-line) is assigned to the first overtone of the D mode. The peak at 1130 cm^{-1} is assigned to the disordered graphite structure (D-line), and the high-frequency peak at ~1580 cm^{-1} (G-line) corresponds to a splitting of the E_{2g} stretching mode of graphite, which reflects the structural intensity of the sp^2-hybridized carbon atoms.[33,34]

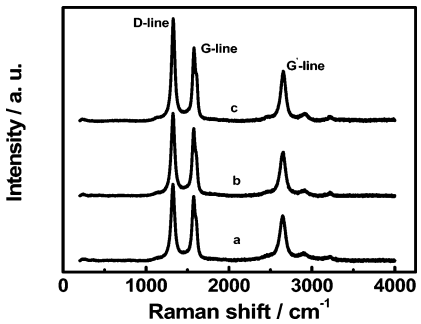

Figure 2. Raman spectra of (a) as-received MWCNTs, (b) MWCNTs treated by H_2O_2/H_2SO_4 solution, and (c) MWCNTs treated by H_2SO_4/HNO_3 solution.

TABLE 1: Surface Area (m^2 g^{-1}) of MWCNTs with Different Tube Diameters before and after the Oxidation Treatment

MWCNTs	as-received	HNO_3/H_2SO_4	H_2O_2/H_2SO_4
<10 nm		310.5	
20−40 nm	88.6	86.4	92.4
40−60 nm		41.0	

Thus the extent of the modification or defect in MWCNTs can be evaluated by the intensity ratio of the D- and G-lines. The intensity ratio of I_D/I_G is 1.1.5, 1.18, and 1.39 for as-received, H_2O_2/H_2SO_4, and H_2SO_4/HNO_3 treated MWCNTs, respectively. MWCNTs treated by H_2O_2/H_2SO_4 and H_2SO_4/HNO_3 solutions have a higher I_D/I_G ratio than that of as-received MWCNTs, indicating the formation of defects or functional groups on MWCNTs after the oxidation treatment.

Since CNTs have a hydrophobic surface, they tend to form aggregates in polar solvents.[21] In order to deposit high loading of metal nanoparticles with uniform distribution, the surface of CNTs needs to be functionalized, e.g., by acid oxidation and sonochemical oxidation treatments.[12,23,35] The significant agglomeration and formation of Pt clusters of Pt/MWCNTs prepared with as-received MWCNTs is most likely due to the hydrophobic and chemically inert surface of carbon nanotubes, which make it difficult for the precursor H_2PtCl_6 to absorb to the surface of MWCNTs. Mu et al.[21] found that oxidation treatment of MWCNTs by H_2SO_4/HNO_3 produced oxygen-containing groups such as carboxylic (−COOH) and carbonyl (−C═O) group. These functional groups modify the hydrophobicity and inertness of the MWCNT surface. This is supported by the observation of the increased I_D/I_G ratio of MWCNTs after the oxidation treatment (Figure 2). As shown by Lordi et al.,[36] these functional sites act as anchors for Pt particles deposited on carbon nanotubes.

Thus, the Pt/MWCNTs prepared with MWCNTs treated by H_2SO_4/H_2O_2 and H_2SO_4/HNO_3 oxidation treatment have a much better distribution and smaller size of Pt particles than that without oxidation treatment (Figure 1b,c). Because the oxidization activity of H_2SO_4/HNO_3 solution is higher than that of H_2SO_4/H_2O_2 solution, there would be more functional groups on the surface of MWCNTs treated in H_2SO_4/HNO_3 than that treated in H_2SO_4/H_2O_2 solution, as indicated by the high I_D/I_G ratio of MWCNTs treated by H_2SO_4/HNO_3 solution (Figure 2). This explains the highly dispersed and very uniform distribution of Pt/MWCNTs synthesized with MWCNTs treated by H_2SO_4/HNO_3 solution (Figure 1c,d). As shown in Table 1, the specific surface area of the MWCNTs does not change significantly with the acid oxidation treatment. This indicates that the acid oxidation treatment would be mainly on the enhancement of the functionality or defects of the MWCNTs. In following

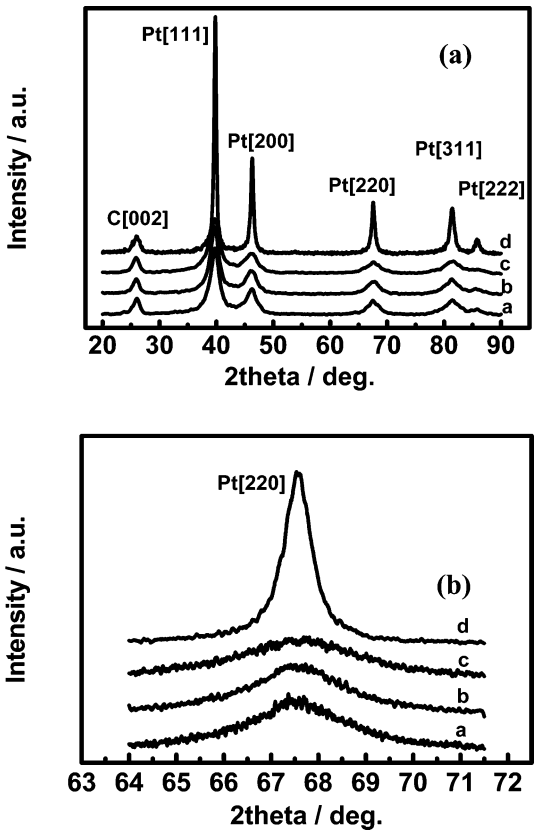

Figure 3. XRD patterns of Pt/MWCNT nanocomposites by different IMI procedures: (a) XRD spectra and (b) Pt(220) peak. Traces a−d: a, Pt/MWCNT-60s; b, Pt/MWCNT-80s; c, Pt/MWCNT-100s; d, Pt/MWCNT-120s.

sections (3.2 to 3.4), Pt/MWCNT nanocomposites were prepared on MWCNTs treated by H_2SO_4/HNO_3 solution.

3.2. Effect of Microwave Heating Procedure. The effect of the intermittent microwave irradiation (IMI) procedure on Pt/MWCNTs with MWCNTs of 20−40 nm tube diameters was studied using four different irradiation procedures, i.e., 10-s irradiation on and 60, 80, 100, and 120-s irradiation off, respectively. The obtained Pt/MWCNT nanocomposites were denoted as Pt/MWCNT-60s, Pt/MWCNT-80s, Pt/MWCNT-100s, and Pt/MWCNT-120s. XRD patterns of the four Pt/MWCNTs are shown in Figure 3. It can be seen that the crystal structure of Pt in the Pt/MWCNT nanocomposites is face-centered cubic (fcc), which is confirmed by the presence of diffraction peaks at 39.6°, 46.3°, 67.4°, 81.4°, and 85.4°.[37] These peaks are assigned to Pt(111), Pt(200), Pt(220), Pt(311), and Pt(222), respectively. This indicates that Pt/MWCNT nanocomposites have been successfully prepared. The average particle size of Pt nanoparticles was 4.0 nm (Pt/MWCNT-60s), 3.8 nm (Pt/MWCNT-80s), 2.9 nm (Pt/MWCNT-100s), and 13.7 nm (Pt/MWCNT-120s), respectively, as determined by Sherrer's formula through line broadening of the Pt(220) peak (Figure 3b). The results indicate that the size of Pt nanoparticles deposited is sensitive to the microwave irradiating procedure.

It is well-known that carbon nanotube is a susceptible carbon material for microwave and can be heated quickly to a high temperature under microwave irradiation.[25] Therefore adjusting microwave irradiation on and off time can effectively control the reaction temperature of the system. Thus, deposition of Pt species to form PtO_x and/or Pt occurs via oxidative thermal treatment under air atmosphere. For the Pt/WMCNTs synthesized using 10-s irradiation on and 120-s irradiation off (Pt/MWCNT-120s), the average crystallite size of Pt nanoparticles was 13.7 nm, significantly larger than those synthesized with shorter irradiation off time. It was also observed that the color of the solution after the thermal treatment turned to yellow with the addition of formic acid, indicating that there was significant amount of unreacted H_2PtCl_6 left in the solution. The reaction temperature may be too low to initiate the nucleation reaction probably due to the long irradiation off period (i.e., 120 s). Thus the grain growth would be kinetically more favorable. On the other hand, short microwave irradiation off time could lead to relatively high temperature of the reaction system, which could accelerate both the nucleation and grain growth reaction for the deposition of Pt nanoparticles. This could be the reason for the relatively larger crystallite size of Pt/MWNCT-60s and Pt/MWCNT-80s in comparison to that of Pt/MWCNT-100s. The particle size of Pt/MWCNTs prepared by different irradiation procedures is given in Table 2. The results show that the procedure of 10-s irradiation on and 100-s irradiation off is adequate to synthesize Pt/MWCNT nanocomposites with uniform distribution and nanosized Pt catalyst.

TABLE 2: Average Crystallite Size of Pt Nanoparticles, Electrochemically Active Area (EAA), Peak Current Density, and Mass Activity for Methanol Oxidation Reaction of Various Pt/MWCNT Nanocomposite Catalysts[a]

Pt/MWCNT catalysts	Pt particle size (nm)	Q_H (mC cm^{-2})	EAA (m^2 g^{-1})	peak current density @ 0.68 V (mA cm^{-2})	mass activity @ 0.68 V (A g^{-1})
as-received MWCNTs	4.2	15.5	31.3	50.5	214.9
MWCNTs by H_2SO_4/H_2O_2	3.5	21.3	43.0	64.0	272.3
MWCNTs by H_2SO_4/HNO_3	2.9	27.5	51.4	90.3	384.3
Pt/MWCNT-60s	4.0	18.8	38.1	61.6	262.1
Pt/MWCNT-80s	3.8	21.6	43.7	71.7	305.2
Pt/MWCNT-100s	2.9	27.5	51.4	90.3	384.3
Pt/MWCNT-120s	13.7	12.5	25.4	40.0	170.2
Pt/MWCNT-10nm	2.9	31.7	64.3	101.0	429.8
Pt/MWCNT-30nm	2.9	27.5	51.4	90.3	384.3
Pt/MWCNT-50nm	4.4	24.1	48.8	74.5	317.0
E-TEK 40% Pt/C	n.a.	20.5	41.5	69.1	294.4

[a] The average size of Pt nanoparticles was obtained by XRD analysis.

3.3. Effect of MWCNT Tube Diameter. To investigate effect of MWCNT tube diameter/surface area on Pt deposition, three MWCNT samples with tube diameter of <10 nm, 20−40 nm, and 40−60 nm were used to synthesize Pt/MWCNTs by the IMI procedure of 10-s irradiation on and 100-s irradiation off (denoted as Pt/MWCNT-10nm, Pt/MWCNT-30nm, and Pt/MWCNT-50nm). The Pt/MWCNT nanocomposites were reduced in the presence of HCOOH as standard.

Figure 4 shows the TEM micrographs of Pt/MWCNT nanocomposites prepared with different MWCNTs. Pt particles were uniformly deposited on the MWCNT-10nm (Figure 4a) and MWCNT-30nm (Figure 4b), and the Pt particle size was in the range of 1.5−4.0 nm. In the case of Pt/MWCNT-50nm, agglomeration and cluster were formed (Figure 4c). XRD analysis showed that the average particle size of both Pt/MWCNT-10nm and Pt/MWCNT-30nm is ∼2.9 nm, but Pt/MWCNT-50nm has a particle size of 4.4 nm. The reason may be related to the surface area of MWCNT supports. As shown in Table 1, the surface area of MWCNT-10nm, MWCNT-30nm, and MWCNT-50nm was 310.5, 86.4, and 41.0 m^2 g^{-1}, respectively.

For the MWCNTs with high surface area (MWCNT-10nm and MWCNT-30nm), there would be a large number of

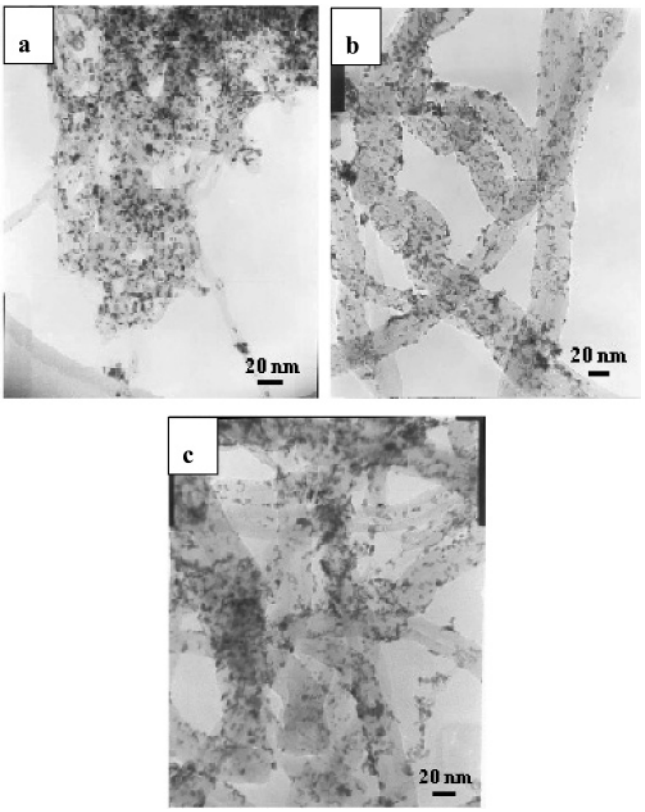

Figure 4. TEM micrographs of (a) Pt/MWCNT-10nm, (b) Pt/MWCNT-30nm, and (c) Pt/MWCNT-50nm.

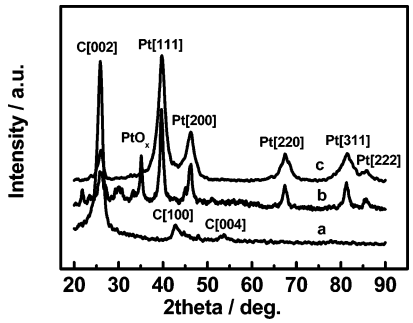

Figure 5. XRD patterns of MWCNTs and Pt/MWCNTs before and after reduction treatment. Traces a−c: a, MWCNTs; b, Pt/MWCNTs before reduction treatment; c, Pt/MWCNTs after reduction treatment.

functional groups/sites for the absorption of H_2PtCl_6 precursor and for the accommodation and nucleation of PtO_x/Pt crystallites. However, in the case of the MWCNT support with low surface area (MWCNT-50nm), there would be competition between the nucleation and crystallite growth of PtO_x/Pt nanoparticles due to the limited sites on the MWCNT surface, resulting in relatively larger particle size and cluster formation. Clearly the appropriate surface area of MWCNT support also plays an important role for the dispersion and particle size of the Pt/MWNCT nanocomposite catalysts synthesized by the intermittent microwave irradiation method (Table 2).

3.4. Reduction Treatment by HCOOH. The XRD patterns of the Pt/MWCNTs before and after reduction treatment in HCOOH are shown in Figure 5. Pt/MWCNTs with MWCNTs of 20−40 nm tube diameters were prepared by the IMI procedure of 10-s irradiation on and 100-s irradiation off. For the purpose of comparison, XRD of pure MWCNTs after the oxidation treatment in H_2SO_4/HNO_3 solution is also shown in the figure. For MWCNTs, the diffraction peaks at 25.9° (d = 3.4371), 42.6° (d = 2.1204), and 53.6° (d = 1.7078) can be

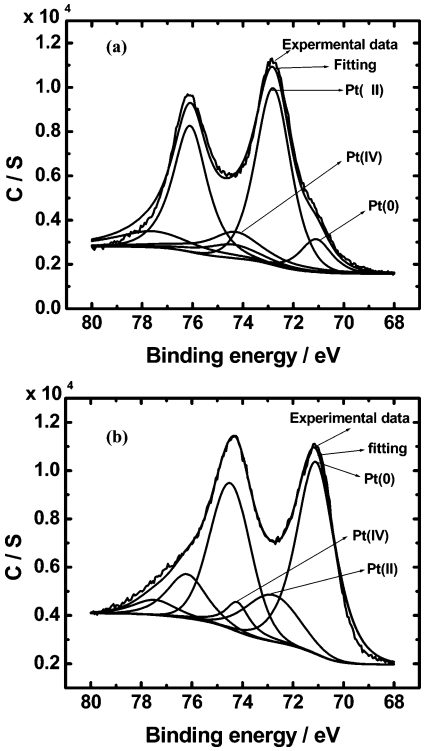

Figure 6. XPS spectrum of the Pt 4f photoemission from the Pt/MWCNT nanocomposite (a) before and (b) after reduction treatment.

assigned to the hexagonal graphite crystallographic planes (002), (100), and (004), respectively, indicating that the MWCNTs used in this study are graphitized carbon. The characteristic diffraction peaks of Pt(0) with a fcc structure are found in the Pt/MWCNT nanocomposites before the reduction treatment, i.e., Pt(111) at 39.6°, Pt(200) at 46.3°, Pt(220) at 67.4°, and Pt(311) at 81.4°. However, a strong diffraction peak was found at 35.08° (2.5558 nm). The standard d-value of PtO_2 is 2.5800 nm (34.74°) and Pt_3O_4 is 2.4980 nm (35.92°). It is believed that the peak at 35.08° results from the overlap of peaks at 34.74° and at 35.92°, because these two peaks are very close. For the Pt/MWCNT nanocomposite after the reduction treatment, the diffraction peak at 35.08° disappears, implying the reduction of platinum oxides to metallic Pt in the presence of formic acid. It is also seen that both Pt/MWCNT nanocomposites before and after reduction treatment have a much lower diffraction intensity of C(002) than that of pure MWCNTs, indicating that the microwave irradiation might have some detrimental effect on the structure of the MWCNTs.

XPS spectra of Pt/MWCNT nanocomposites before and after the reduction treatment are shown in Figure 6. For Pt/MWCNTs before the reduction treatment, the XPS spectra are characterized by a doublet containing a binding energy (BE) of 72.85 eV (Pt $4f_{7/2}$) and 76.2 eV (Pt $4f_{5/2}$) (Figure 6a). The two peaks have a binding energy difference of 3.35 eV and a peak area ratio of 4:3, which corresponds to the characteristics of the Pt4f(II). This indicates that the majority of Pt species in Pt/MWCNT nanocomposites exist as Pt(II) before the reduction treatment. The Pt 4f spectrum can be deconvoluted into three species with BE of 71.1−74.4, 72.8−76.1, and 74.3−77.6 eV, which correspond to Pt(0), Pt(II), and Pt(IV), respectively. On the basis of the areas of Pt $4f_{7/2}$, the relative intensity of Pt(0), Pt(II), and Pt(IV) was calculated to be 11.4%, 67.8%, and 20.8%, respectively. This indicates that the Pt oxides in the Pt/MWCNTs before the reduction would be primarily PtO and PtO_2, which is in general consistent with that of XRD analysis. The presence

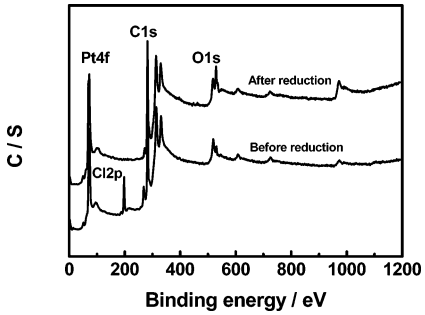

Figure 7. XPS survey scan spectra of Pt/MWCNT nanocomposites before and after reduction treatment.

TABLE 3: Distribution of Pt Species in the Pt/MWCNT Nanocomposites before and after the Reduction Treatment

		binding energy(eV)		
Pt/MWCNTs	Pt species	Pt $4f_{7/2}$	Pt $4f_{5/2}$	rel density (%)
before reduction	Pt(0)	71.1	74.4	11.4
	Pt(II)	72.8	76.1	67.8
	Pt(IV)	74.3	77.6	20.8
after reduction	Pt(0)	71.1	74.5	70.5
	Pt(II)	72.8	76.2	21.5
	Pt(IV)	74.2	77.5	8.0

of a relatively small percentage of Pt(0) indicates the partial reduction of PtO_x during the intermittent microwave irradiation, probably due to the CO produced under high temperature. CO produced could serve as reducing agency to partially reduce PtO_x.

The XPS patterns of the Pt/MWCNTs after reduction treatment are represented by the binding energies of Pt $4f_{7/2}$ and Pt $4f_{5/2}$ at 71.1 eV and 74.4 eV, respectively, characteristic BE of Pt(0) (Figure 6b). This shows that most of the PtO_x in the Pt/MWCNTs after the reduction treatment in formic acid has been reduced to metallic Pt. This is supported by the analysis of the XPS spectrum, showing the relative intensity of 70.5%, 20.5%, and 8.0% for Pt(0), Pt(II), and Pt(IV), respectively. The XPS characterization shows that Pt/MWCNT nanocomposites synthesized by the IMI method have oxidation states of Pt similar to those prepared by other methods.[17] The results of the XPS analysis of the Pt/MWCNTs before and after reduction treatment are summarized in Table 3.

Besides the Pt 4f spectrum, a survey XPS scan was also carried out on Pt/MWCNT nanocomposites before and after reduction treatment (Figure 7). It can be seen that peaks of Pt 4f, Cl 2p, C 1s, and O 1s exist in the Pt/MWCNT nanocomposite before the reduction. However, the Cl 2p peak vanished for the reduced Pt/MWCNT sample, indicating removal of chloride ion in the phase of reduction. The removal of halide ion impurities such as Cl^- can improve the catalytic activity of the catalyst for CO oxidation and is beneficial for direct methanol fuel cells.[38,39]

On the basis of the above XRD and XPS analysis, reaction steps for the synthesis of Pt/MWCNT nanocomposites by the IMI method can be written as follows:

Step 1. The $PtCl_6^{2-}$ ions of precursor H_2PtCl_6 anchored to the surface of the acid-treated MWCNTs are oxidized into PtO and PtO_2 by intermittent microwave irradiation thermal treatment.

$$PtCl_6^{2-} + (x/2)O_2 \rightarrow PtO_x + 2HCl + 2Cl_2 \qquad (x = 1, 2) \tag{2}$$

At the same time carbon monoxide could be formed under high temperature due to the microwave irradiation, and subsequently part of PtO_x is reduced by CO.

$$C + (1/2)O_2 \rightarrow CO \tag{3}$$

$$PtO_x + xCO \rightarrow Pt + xCO_2 \tag{4}$$

Step 2. PtO and PtO_2 in the Pt/MWCNTs are reduced in the presence of HCOOH by reflux.

$$PtO_x + xHCOOH \rightarrow Pt + xCO_2 + xH_2O \tag{5}$$

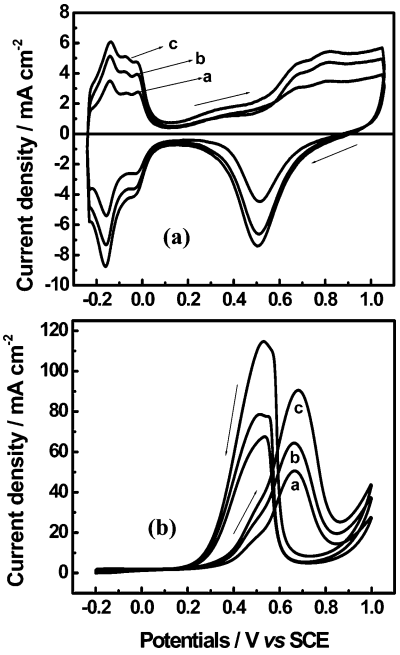

Figure 8. Cyclic voltammograms of Pt/MWCNT nanocomposites prepared on MWCNT support with different treatments in (a) nitrogen saturated 0.5 M H_2SO_4 and (b) nitrogen saturated 0.5 M H_2SO_4 + 1 M CH_3OH. Traces a−c: a, as-received MWCNTs; b, MWCNTs treated by H_2SO_4/H_2O_2; c, MWCNTs treated by H_2SO_4/HNO_3.

3.5. Electrochemical Performance of Pt/MWCNT Nanocomposites. Cyclic voltammograms (CVs) of Pt/MWCNTs synthesized with MWCNTs pretreated in different acid solutions measured in nitrogen saturated 0.5 M H_2SO_4 and 0.5 M H_2SO_4 + 1 M CH_3OH solutions are shown in Figure 8. Well-defined CVs are obtained in all Pt/MWCNT samples in both solutions. In the CVs obtained in 0.5 M H_2SO_4 electrolyte solution (Figure 8a), the cathodic and anodic peaks appearing between −0.20 and 0.10 V originate from the adsorption and desorption of atomic hydrogen in acidic media. Thus the area of H-adsorption or H-desorption on the CV curve can be used to estimate the electrochemical activity area (EAA) of Pt catalysts.[40,41] By using the charge passed for H-desorption Q_H, EAA can be calculated according to the following equation:

$$EAA = Q_H/L_{Pt} \times 0.21 \tag{6}$$

in which L_{Pt} represents the platinum loading (mg cm^{-2}) in the electrode and 0.21 (mC cm^{-2}) is the charge required to oxidize a monolayer of H_2 on a bright Pt. The calculated EAA data of Pt/MWCNT nanocomposites prepared on MWCNTs with different oxidation treatments are also given in Table 2.

For Pt supported on as-received MWCNTs, the EAA is 31.3 $m^2\ g^{-1}$, and for Pt supported on H_2SO_4/H_2O_2 and H_2SO_4/HNO_3 treated MWCNTs, the EAA is 43.0 and 51.4 $m^2\ g^{-1}$, respectively. Pt/MWCNTs synthesized with H_2SO_4/HNO_3 treated MWCNTs have the highest electrochemically active surface area

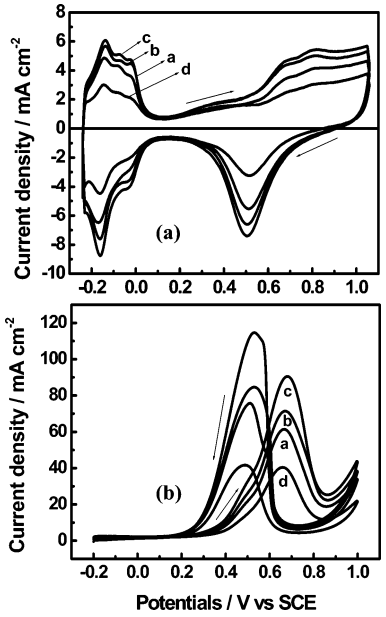

Figure 9. Cyclic voltammograms of Pt/MWCNT nanocomposites prepared by different intermittent microwave irradiation process in (a) nitrogen saturated 0.5 M H_2SO_4 and (b) nitrogen saturated 0.5 M H_2SO_4 + 1 M CH_3OH. Traces a−c: a, Pt/MWCNT-60s; b, Pt/MWCNT-80s; c, Pt/MWCNT-100s; d, Pt/MWCNT-120s.

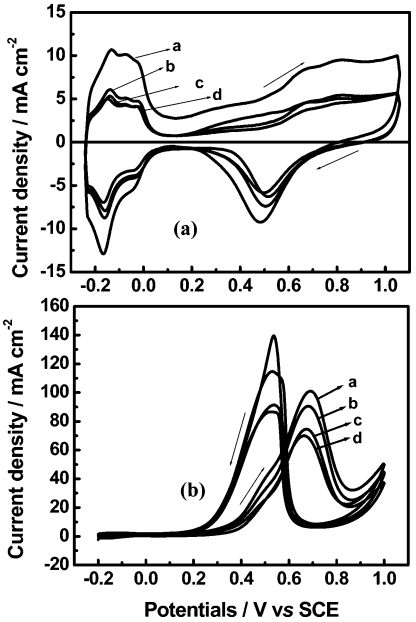

Figure 10. Cyclic voltammograms of Pt/MWCNT nanocomposites prepared on MWCNTs with different diameters in (a) nitrogen saturated 0.5 M H_2SO_4 and (b) nitrogen saturated 0.5 M H_2SO_4 + 1 M CH_3OH. Traces a−d: a, Pt/MWCNT-10nm; b, Pt/MWCNT-30nm; c, Pt/MWCNT-50nm; d, E-TEK 40% Pt/C.

most likely due to the uniform distribution and small size of Pt nanoparticles (2.9 nm, see Table 2).

The catalytic properties of Pt supported on MWCNTs treated by different acid solutions for methanol oxidation reaction were characterized by cyclic voltammetry obtained in a nitrogen saturated 0.5 M H_2SO_4 + 1 M CH_3OH solution (Figure 8b). The Faradaic current exhibits the well-known dependence on the electrode potential typical for the methanol oxidation reaction on a carbon nanotube or carbon-supported Pt catalyst.[26,42,43] Methanol oxidation is represented by the anodic peak around 0.68 V. In the reverse scan, the adsorbed intermediates produce a second oxidation peak at ~0.53 V. The magnitude of the peak current at 0.68 V is directly proportional to the amount of methanol oxidized at the Pt/MWCNT nanocomposite electrode. The Pt supported on MWCNTs treated by H_2SO_4/HNO_3 shows a highest methanol oxidation current, and the peak current is 90.3 mA cm^{-2}, which is 72.3% higher than Pt supported on as-received MWCNTs (50.5 mA cm^{-2}). The high electrocatalytic activity of Pt/MWCNTs prepared on H_2SO_4/HNO_3 treated MWCNTs agrees well with the small particle size and high electrochemically active area of the catalyst. The mass specific activity of the Pt/MWCNT nanocomposites is also given in Table 2.

Figure 9 shows the cyclic voltammograms of Pt/MWCNT nanocomposites prepared by different IMI procedures obtained in nitrogen saturated 0.5 M H_2SO_4 and 0.5 M H_2SO_4 + 1 M CH_3OH solutions. Pt/MWCNTs prepared by different IMI procedures have different hydrogen adsorption−desorption currents, indicating that the electrochemically active area of Pt/MWCNTs depends strongly on the microwave irradiation procedure (Figure 9a). Pt/MWCNT nanocomposite synthesized by the procedure of 10-s irradiation on and 100-s irradiation off (Pt/MWCNT-100s) has the highest electrochemically active area (51.4 m^2 g^{-1}) in comparison to other microwave irradiation procedures (see Table 2). Similarly the highest activity for the methanol oxidation was observed on the Pt/MWCNT-100s nanocomposite catalyst. The mass activity of Pt/MWCNT-100s was 384.3 A g^{-1} at 0.68 V, which is more than double of the value of 170.2 A g^{-1} obtained for the reaction on Pt/MWCNT-120s. The catalytic activity of the Pt/MWCNT nanocomposite for the methanol oxidation follows the order Pt/MWCNT-100s > Pt/MWCNT-80s > Pt/MWCNT-60s > Pt/MWCNT-120s. As shown in Figure 3, the average particle size of Pt in Pt/MWCNT-100s is 2.9 nm, smallest among the Pt/MWCNTs synthesized by different irradiation procedures. This indicates that the electrocatalytic activity of the Pt/MWCNT nanocomposites for the methanol oxidation reaction depends strongly on the particle size of dispersed Pt nanoparticles.

The electrocatalytic properties of Pt supported on MWCNTs with different tube diameters are also investigated by cyclic voltammetry in nitrogen saturated 0.5 M H_2SO_4 and 0.5 M H_2SO_4 + 1 M CH_3OH solutions (Figure 10). In the figure the catalytic activity of an E-TEK 40% Pt/C catalyst is given for the purpose of comparison. The Pt/MWCNT nanocomposites supported on MWCNTs with different diameters have higher or comparable faradaic current in the electrode potential region for the hydrogen adsorption−desorption process in comparison to the commercial E-TEK catalyst, implying that the Pt/MWCNTs prepared by the intermittent microwave irradiation method have high electrochemical activity area. Pt supported on MWCNTs with a diameter of <10 nm (Pt/MWCNT-10nm) has the highest hydrogen adsorption−desorption current and thus the highest electrochemical surface area (Table 2). Not surprisingly, Pt/MWCNT-10nm nanocomposite has the highest electrocatalytic activity for the methanol oxidation reaction (Figure 10b). The mass specific current was 429.8 A g^{-1} for the methanol oxidation reaction on Pt/MWCNT-10nm nanocomposite catalyst, which is significantly higher than 294.4 A g^{-1} obtained on the E-TEK 40% Pt/C catalyst under the same experimental conditions. This demonstrates the high catalytic activities of the Pt catalyst supported on MWCNTs synthesized by the IMI method.

Besides a uniform heating process, the microwave synthesis approach allows the possibility to scale-up production without compromising the quality and the yield of the synthesized nanocomposites. The significant effect of the intermittent

microwave irradiation procedure on the average crystalline size of Pt nanoparticles (see Figure 3 and Table 2) indicates that intermittent microwave irradiation is effective to control the particle size of a Pt catalyst. On the other hand, the remarkable dependence of the dispersion of Pt nanoparticles on the oxidation treatment and the diameter of MWCNT support demonstrates the critical role of the geometric factor of the support in the catalytic activity of Pt based catalyst. The present study shows that uniformly dispersed Pt nanoparticles with size less than 3 nm and sufficiently high metal catalyst loading (40 wt % or higher) can be easily achieved with the intermittent microwave irradiation method, using specific MWCNTs.

4. Conclusion

The intermittent microwave irradiation technique provides a simple and rapid method for the synthesis of Pt/MWCNT nanocomposite with high electrocatalytic activity for methanol oxidation in H_2SO_4 solutions. The dispersion and size of Pt nanoparticles in Pt/MWCNT nanocomposites are remarkably affected by the oxidation treatment of MWCNTs, the intermittent microwave irradiation procedure, and the MWCNT tube diameter. Pt/MWCNTs with extremely uniform distribution of the Pt nanoparticles and particle size less than 3 nm were synthesized by the intermittent microwave irradiation method. However, it is necessary to treat the synthesized Pt/MWCNT nanocomposites in formic acid to reduce PtO_x to metallic Pt as shown by the detailed XPS and XRD analysis. The Pt/MWCNT nanocomposites synthesized show significantly higher electrochemically active area and higher catalytic activities toward the methanol oxidation reaction as compared to a commercial E-TEK 40% Pt/C catalyst.

References and Notes

(1) Mehta, V.; Cooper, S. J. *J. Power Sources* **2003**, *114*, 32.
(2) Ralph, T. R.; Hogarth, M. P. *Platinum Metals Rev.* **2002**, *46*, 3.
(3) Hogarth, M. P.; Munk, J.; Shukla, A. K.; Hamnett, A. J. *J. Appl. Electrochem.* **1994**, *24*, 85.
(4) Ralph, T. R.; Hards, G. A.; Keating, J. E.; Campbell, S. A.; Wilkinson, D. P.; Davis, M.; St-Pierre, J.; Johnson, M. C. *J. Electrochem. Soc.* **1997**, *144*, 3845.
(5) Gloaguen, F.; Leger, J. M.; Lamy, C. *J. Appl. Electrochem.* **1997**, *27*, 1052.
(6) Niu, C.; Sichel, E. K.; Hoch, R. *Appl. Phys. Lett.* **1997**, *7*, 1480.
(7) Ma, R. Z.; Liang, J.; Wei, B. Q. *J. Power Sources* **1999**, *84*, 126.
(8) Dillon, A. C.; Jones, K. M.; Bekkedahl, T. A.; Kiang, C. H.; Bethune, D. S.; Heben, M. J. *Nature* **1997**, *386*, 377.
(9) Wang, Q. H.; Setlur, A. A. Lauerhaas, *Appl. Phys. Lett*. **1998**, *72*, 2912.
(10) Fan, S.; Chapline, M. G.; Franklin, N. R. *Science* **1999**, *283*, 215.
(11) Cheng, H. M.; Yang Q. H.; Liu C. *Carbon* **2001**, *39*, 1447.
(12) Che, G.; Lakshmi, B. B.; Martin, C. R.; Fisher, E. R. *Langmuir* **1999**, *15*, 750.
(13) Steigerwalt, E. S.; Deluga, G. A.; Cliffel, D. E. *J. Phys. Chem. B* **2001,** *105*, 8097.
(14) Carmo, M.; Paganin, V. A.; Rosolen, J. M.; Gonzalez, E. R. *J. Power Sources* **2005**, *142*, 169.
(15) Rajesh, B,; Thampi, K. R.; Bonard, J. M.; Xanthopoulos, N.; Mathieu, H. J.; Viswanathan, B. *J. Phys. Chem. B* **2003**, *107*, 2701.
(16) Taketoshi, M.; Toshiki K.; Kazuya A.; Takahisa, Y.; Masashi, K.; Harukazu, S.; Yosuke, T.; Junji, N. *Chem. Commun*. **2004**, *7*, 840.
(17) Liu, Z.; Lin, X.; Lee, J. Y.; Zhang, W.; Han, M.; Gan, L. M. *Langmuir* **2002**, *18*, 4054.
(18) Li, W. Z.; Liang, C. H.; Zhou, W. J. Qiu, J. S.; Zhou, Z. H.; Sun, G. Q.; Xin, Q. *J. Phys. Chem. B* **2003**,*107*, 6292.
(19) Li, W. Z.; Liang, C. H.; Zhou, W. J. J.; Sun, G. Q.; Xin, Q. *Carbon* **2004**, *42*, 423.
(20) Chen, W. X.; Lee, J. Y., Liu, Z. L. *Mater. Lett.* **2004**, *58*, 3166.
(21) Mu, P.; Haolin, T.; Shichun, M.; Runzhang, Y. *J. Mater. Res.* **2005**, *19*, 2279.
(22) Tang, H.; Chen, J. H.; Huang, Z. P.; Wang, D. Z.; Ren, Z. F.; Nie, L. H.; Kuang, Y. F.; Yao, S. Z. *Carbon* **2004**, *42*, 191.
(23) Han, K. L.; Lee, J. S.; Park, S. O.; Lee, S. W.; Park, Y. W.; Kim, H. *Electrochim. Acta* **2004**, *50*, 791.
(24) Lin, Y.; Cui, X.; Yen, C.; Wai, C. M. *J. Phys. Chem. B* **2005**, *109*, 14410.
(25) Boxall, D. L.; Deluga, G. A.; Kenik, E. A.; King, W. D.; Lukehart, C. M. *Chem. Mater.* **2001**, *13*, 891.
(26) Liu, Z.; Ling, X. Y.; Su, X.; Lee, J. Y. *J. Phys. Chem. B* **2004**, *108*, 8234.
(27) Tian, Z. Q.; Xie, F. Y.; Shen, P. K. *J. Mater. Sci.* **2004**, *39*, 1509.
(28) Shen, P. K.; Tian, Z. Q. *Electrochim. Acta* **2004**, *49*, 3107.
(29) Meng, H.; Shen, P. K. *Chem. Commun*. **2005**, *35*, 4408.
(30) Xu, C. W.; Shen, P. K. *Chem. Commun*. **2004**, *19*, 2238.
(31) Yu, R. Q.; Chen, L. W.; Liu, Q. P. Lin, J. Y.; Tan, K. L.; Ng, S. C.; Chan, H. S. O.; Xu, G.-Q.; Hor, T. S. A. *Chem. Mater*. **1998**, *10*, 718.
(32) Antolini, E.; Cardellini, F. *J. Alloys Comp*. **2001**, *315*, 118.
(33) Dresselhaus, M. S.; Dresselhaus, G.; Saito, R.; Jorio, A. *Phys. Rep.* **2005**, *109*, 47.
(34) Belin, T.; Epron, F. *Mater. Sci. Eng. B* **2005**, *119*, 105.
(35) Xing, Y.; Li, L.; Chusuei, C. C.; Hull, R. V. *Langmuir* **2005**, *21*, 4185.
(36) Lordi, V.; Yao, N.; Wei, J. *Chem. Mater.* **2001**, *13*, 733.
(37) Fujiwara, N.; Yasuda, K.; Ioroi, T.; Siroma, Z.; Miyazaki, Y. *Electrochim. Acta* **2002**, *47*, 4079.
(38) Strmcnik, D.; Gaberscek, M.; Hocevar, S.; Jamnik, J. *Solid State Ionics* **2005**, *176*, 1759.
(39) Zhao, X.; Sun, G.; Jiang, L.; Chen, W.; Tang, S.; Zhou, B.; Xin, Q. *Electrochem. Solid-State Lett.* **2005**, *8*, A149.
(40) Perez, J.; Gonzalez, E. R.; Ticianelli, E. A. *Electrochim. Acta* **1998**, *44*, 1329.
(41) Pozio, A.; Francesco, M. D.; Cemmi, A.; Cardellini, F.; Giorgi, L. *J. Power Sources* **2002**, *105*, 13.
(42) Jusys, Z.; Kaiser, J.; Behm, R. J. *Langmuir* **2003**, *19*, 6759.
(43) Girishkumar, G.; Vinodgopal, K.; Kamat, P. V. *J. Phys. Chem. B* **2004**, *108*, 19960.